

FUNCTIONALIZATION OF PEDOT NANOPARTICLES FOR TARGETED  
DELIVERY TO CANCER CELLS

by

Lillian Noel Roe

HONORS THESIS

Submitted to Texas State University  
in partial fulfillment  
of the requirements for  
graduation in the Honors College  
December 2021

Thesis Supervisor:

Tania Betancourt

Second Reader:

Jennifer Irvin

## ACKNOWLEDGEMENTS

I have many people to thank who have supported and guided me throughout the six months that this research took place. I would like to start off with a huge expression of gratitude to my research advisor, Dr. Tania Betancourt. Working under her has been an absolute privilege, and I could not have asked for a more kind, supportive, and patient mentor to introduce me to the ups and downs of research. Prior to starting work in the Betancourt lab, I felt a lot of impostor syndrome surrounding my ability to succeed as a scientist, but Dr. Betancourt has helped me realize my potential and I will always be so thankful for the opportunities she has opened up for me. I would also like to thank my second reader, Dr. Jennifer Irvin. Her inputs into this project and thesis have been very valuable and I have learned so much from her even after only a short time working together.

I am also very appreciative of the support of all of my labmates through this process. I would specifically like to thank Dami Runsewe, Emilio Lara, Wasan Al-Sammarraie, and Marvin Santiago for training me and being wonderful teachers. I would also like to specifically thank labmates Grace Haya, Joanna Zepeda, and Kobe De La Paz. In addition, I want to extend a thank you to all those involved in facilitating the TXST SURE program (U.S. Department of Education HSI STEM program (841.031c), Award #P021C160036) and the NSF PREM program (NSF Grant DMR-2122041). Both of these programs have provided funding for this work and provided opportunities for my professional development that I appreciate.

I would like to thank my co-workers at the TXST University Writing Center for

their support during this process, and especially Johnny Dao for reading and improving my thesis. I would like to thank my mom and my brother for supporting me and being willing to listen to me talk about science even when they may have no idea what anything I'm saying means. Finally, I would like to thank my good friend José Milán for being my rock through the thesis process and through my experience at TXST in general—thank you for pushing me to succeed but also knowing just how to make me laugh and feel better when I was pushing myself too hard. I couldn't have done it without you!

## TABLE OF CONTENTS

	Page
ACKNOWLEDGEMENTS.....	2
LIST OF FIGURES.....	5
ABSTRACT.....	6
CHAPTER	
1. INTRODUCTION.....	7
1.1. Project Overview.....	7
1.2. Cancer and PTT.....	7
1.3. Nanomaterials in PTT.....	9
1.4. Altered Protein Expression in Cancer & Targeting Molecules.....	12
1.5. PEDOT Nanoparticle Functionalization.....	14
2. MATERIALS & METHODS.....	15
2.1. Materials.....	15
2.2. PEDOT Nanoparticle Synthesis & Characterization.....	16
2.3. Carbodiimide Functionalization.....	18
2.4. Layer-by-Layer Assembly Functionalization.....	22
2.5. Ionic Linking to PAH-Coated PEDOT Nanoparticles.....	24
2.6. Covalent Linking to PAH-Coated PEDOT Nanoparticles Using SC-PEG-CM.....	24
3. RESULTS & DISCUSSION.....	26
3.1. PEDOT Nanoparticle Synthesis & Characterization.....	26
3.2. Carbodiimide Functionalization.....	28
3.3. Layer-by-Layer Assembly Functionalization.....	31
3.4. Ionic Linking to PAH-Coated PEDOT Nanoparticles.....	33
3.5. Covalent Linking to PAH-Coated PEDOT Nanoparticles Using SC-PEG-CM.....	34
4. CONCLUSIONS & FUTURE WORK.....	36
REFERENCES.....	40
APPENDICES.....	43

## LIST OF FIGURES

<b>Figure</b>	<b>Page</b>
1. PEDOT Nanoparticle Synthesis.....	17
2. Schematic of Carbodiimide Functionalization Method.....	21
3. Schematic of PAH Layering Onto PEDOT Nanoparticles.....	23
4. Schematic of Ionic Attachment of Aptamer to PAH-Coated PEDOT Nanoparticles...	24
5. Schematic of Covalent Linking to Aptamer Using SC-PEG-CM.....	26
6. Size Distribution of PEDOT Nanoparticles.....	27
7. Absorption Spectrum of PEDOT Nanoparticles.....	28
8. Absorbance of PEDOT Nanoparticles Conjugated to BSA-FITC.....	29
9. Fluorescence of PEDOT Nanoparticles Conjugated to BSA-FITC.....	30
10. Zeta Potential of PEDOT Nanoparticles Conjugated to BSA-FITC.....	31
11. Zeta Potential of PAH-Coated PEDOT Nanoparticles.....	32
12. Zeta Potential of Nanoparticles With Ionically Attached Aptamer.....	34
13. Zeta Potential of Nanoparticles After PEG Attachment.....	35
14. Zeta Potential of Nanoparticles After Covalent Aptamer Attachment.....	36

## ABSTRACT

Nanoparticle-mediated photothermal therapy uses nanoparticles as photothermal agents to harness light energy and convert it to thermal energy to locally heat and damage or kill cancer cells. Previous studies in our research group have shown that poly(3,4-ethylenedioxythiophene) nanoparticles (PEDOT NPs) are effective photothermal agents and have the ability to mediate cancer cell death upon irradiation with a near-infrared laser. In order to make cancer treatment with PEDOT NPs more effective and selective, functionalization of the NPs is needed to ensure targeted binding to cancer cell receptors. In this work, we evaluate different methods of PEDOT NP functionalization with aptamers. The aim of this research is to develop a versatile functionalization method that can be used to attach many different targeting molecules to PEDOT NPs.

# 1. INTRODUCTION

## 1.1. Project Overview

Cancer is one of today's leading causes of death, and current treatment methods come with many drawbacks and side effects. One newly explored treatment method for cancer is nanoparticle-mediated photothermal therapy. Within the concept of nanoparticle-mediated photothermal therapy, a problem to be addressed is nonspecificity. One way to counteract this is to functionalize the nanoparticles with a targeting molecule to encourage them to locate and bind specifically to the tumor cells of interest. This study attempts to solve the problem of nonspecificity by investigating different functionalization methods that could be used to facilitate targeted delivery of nanoparticles to tumor tissues for nanoparticle-mediated photothermal therapy of cancer.

## 1.2. Cancer and PTT

According to the American Cancer Society, there will be an estimated 1.9 million new cases of cancer diagnosed in the U.S. in 2021, with 608,570 of these cases estimated to be fatal.<sup>1</sup> The prevalence of cancer makes it the second leading cause of death in the United States, with the number one cause being cardiovascular disease and number three now being COVID-19.<sup>2,3</sup> The most common treatments used to treat late-stage cancer are radiation, chemotherapy, and surgery, all of which come at the cost of also harming non-cancerous tissues in the body. Chemotherapeutic drugs target fast-replicating cells such as cancer cells, but during treatment these drugs travel throughout the body and affect fast-replicating healthy cells in addition to the targeted cancer cells. The healthy

fast-replicating cells most commonly affected by chemotherapy are blood-forming cells in the bone marrow, hair follicles, and cells in the mouth, digestive tract, and reproductive system.<sup>4</sup> The damage to these cells leads to adverse side effects for the patient. In addition, these cancer treatment methods often have low efficacy in completely eliminating the cancer, enabling cancer recurrence. The prevalence of cancer and the drawbacks associated with its current most common treatment methods call for the exploration of alternative approaches to cancer therapy.

One newly explored method that may have promise in the treatment of cancer is hyperthermia. In the context of cancer treatment, hyperthermia describes the use of heat as a method of damaging or killing cancer cells. High heat can cause damage to essential proteins within the cell, causing them to denature and be unable to perform their normal function.<sup>5</sup> In addition, extreme heat can directly ablate and kill the cells. Aside from disrupting the normal functioning of cancer cells physically, heating can make cells more vulnerable to eradication by the human immune system.<sup>5</sup> Hyperthermia can also facilitate better delivery of chemotherapeutic drugs by increasing blood flow to the cancerous tissue and sensitizing the cells to induce higher effectivity of the drugs.<sup>5</sup>

A specific form of hyperthermia that is being explored as cancer therapy is photothermal therapy (PTT). PTT involves the integration of a material with photothermal properties into the tumor area which can then be irradiated with an external laser source to induce in situ photothermal conversion and thereby localized hyperthermia. Photothermal conversion involves conversion of energy in the form of light into energy in the form of heat. Light exists at a variety of different wavelengths,

and is classified into different categories based on the energy of the wavelengths. Infrared (IR) light describes the range of light found just higher in energy than what is visible to the human eye. Near-infrared (NIR) light is light within the range of about 700 nanometers to 1000 nanometers. NIR radiation is of interest for use in PTT because it is the range of light that best penetrates the body without being absorbed.<sup>6</sup> Higher energy forms of light are absorbed by the body's tissues, potentially causing damage, while lower energy forms of light can be absorbed by water and lipids and would not be effective in carrying enough energy to be converted to an effective amount of heating through PTT.

### **1.3. Nanomaterials in PTT**

Photothermal agents that have been explored in the use of PTT largely consist of nanomaterials such as gold- or silver- based nanostructures such as nanoshells, nanorods, and nanoparticles. These metal nanostructures are effective photothermal agents because they have strong absorption in the NIR range and fast energy conversion and dissipation.<sup>7</sup> In practice, nanostructure-mediated PTT after the diagnosis of cancer would first involve the administration of a photothermal material, most often photothermal nanostructures, to the affected area. This could be achieved by using ultrasound to guide needle insertion into tumors. Alternatively, the nanostructures could be administered systematically through intravenous injection and allowed to accumulate at the tumor site prior to irradiation. Next, the nanostructures would need to localize and bind to the tumor cells.

Once bound, the nanostructures could be locally irradiated with a NIR laser. This would cause hyperthermia within the cells, damaging or killing them.

The heating of gold nanostructures has been shown to cause irreversible cell destruction through the various methods associated with hyperthermia.<sup>7</sup> In addition, the heating of these structures has been shown to vaporize a thin layer of water that surrounds them, leading to increased cell damage and death.<sup>7</sup> Gold nanoshell PTT has reached the clinical stage, with ongoing clinical trials being conducted. Several pilot studies have been conducted using AuroLase™ therapy--photothermal therapy using AuroShell particles--for ablation of various types of cancers.<sup>8,9</sup> The AuroShell particles were designed by Nanospectra Biosciences and they consist of a gold shell and a silica core with a diameter of about 150 nm, absorption in the NIR range, and photothermal conversion ability.<sup>9</sup> One study on the treatment of prostate cancer in men showed that ablation of the cancer occurred in 94% of patients tested, and follow-up showed no significant side effects.<sup>9</sup> Because PTT using gold nanostructures has shown promise as a method of cancer treatment, PTT using other types of photothermal materials have also been explored, including carbon nanomaterials, prussian blue nanoparticles, metal-organic frameworks, and polymeric nanoparticles loaded with small molecule chromophore photothermal agents.<sup>10,11,12,13</sup>

Another type of material that has been recently explored for use in PTT is conductive polymer nanoparticles. Polymers are large molecules consisting of repeating subunits called monomers. Conductive polymers are unique in that they have the ability to conduct electricity due to their conjugated structure. Conjugation describes delocalized

electrons shared between alternating double bonds within a molecule. In polymers, conjugation describes when the backbone of the polymer consists of alternating single and double bonds.

Poly(3,4-ethylenedioxythiophene) (PEDOT) nanoparticles are spherical conductive polymer nanoparticles of about 30-80 nm in diameter that absorb light in the NIR range and exhibit photothermal conversion properties. These PEDOT nanoparticles are attractive for PTT for several reasons. First, they are significantly more inexpensive and easier to store than gold-based nanostructures. While commercially available gold nanoparticles are priced at about \$120 for 25 mL and gold nanorods are about \$440 for 24 mL, PEDOT nanoparticles are inexpensive to prepare in large batches. In addition, gold nanostructures are less stable for storage: they must be refrigerated, and they tend to aggregate within a few months. PEDOT nanoparticles, on the other hand, can be stored at room temperature and are very resistant to aggregation. Next, PEDOT nanoparticles have a higher photothermal conversion efficiency than gold nanostructures. The photothermal conversion efficiency of PEDOT nanoparticles is about 53%, while the efficiency for gold nanostructures is about 30%.<sup>14</sup> Finally, PEDOT nanoparticles are highly photostable when compared to gold nanostructures. Gold nanostructures tend to change morphology when heated up too much, and this change in morphology will affect their absorption and ability to heat upon irradiation. PEDOT nanoparticles, however, can be irradiated with a laser multiple times without having any change in morphology or photothermal conversion ability.<sup>14</sup>

PEDOT nanoparticles have shown to be successful in causing death of cancer cells. Our research group has previously demonstrated this by first internalizing PEDOT nanoparticles into MDA-MB-231 breast cancer cells and then irradiating with an NIR laser.<sup>15</sup> At a 500  $\mu\text{g/mL}$  concentration, PEDOT nanoparticles were shown to be able to cause a maximum temperature change of  $32^\circ\text{C}$ , which was sufficient to cause total cell death after 5-15 minutes of NIR laser irradiation. In addition to being able to directly kill the tumor cells, PEDOT nanoparticle-mediated PTT was shown to induce immunogenic cell death in breast cancer cells by increasing the release of damage-associated molecular patterns (DAMPs).<sup>15</sup> This mechanism of cell death and the release of signaling molecules makes it more likely that the patient's immune system will be able to identify and eliminate tumor cells.

#### **1.4. Altered Protein Expression in Cancer & Targeting Molecules**

As previously mentioned, one problem with nanoparticle-mediated photothermal therapy is its nonspecificity; the photothermal nanoparticles can cause cell death in cancerous cells, but without a way to ensure targeted delivery, they may also be internalized into healthy cells and cause them to die or be damaged. In order to address this problem, we can take advantage of the fact that when compared to healthy cells, cancerous cells have altered expression of certain proteins on their membranes. For example, in healthy cells, a membrane-bound glycoprotein called Mucin 1 is normally expressed at low levels and serves the purpose of defending against pathogens.<sup>16</sup> In breast cancer cells, Mucin 1 is significantly overexpressed, meaning that there is more of this

glycoprotein found on the surface of cancerous cells than there is on healthy cells.<sup>17</sup> This upregulation helps the cancerous cells evade detection by the immune system.<sup>17</sup>

Molecules such as antibodies and aptamers are targeting agents that are able to specifically bind to a target molecule. Both antibodies and aptamers are highly versatile and bind to their targets with high selectivity and specificity. Antibodies are proteins commonly found in the blood that contain a variable region that recognizes a specific molecule called an antigen. Antibodies have a large history of usage in research, but the disadvantage of using antibodies for scientific studies is that they are only created in live immune cells, and therefore must be collected from animal serum or from hybridoma cell lines. Another type of targeting molecule, the aptamer, is sometimes referred to as a “chemical antibody”.<sup>18</sup> Aptamers are short single-stranded DNA or RNA molecules that fold to a specific shape and bind to targets such as proteins or peptides. Aptamers can be identified through an *in vitro* process called the Systematic Evolution of Ligands by EXponential enrichment (SELEX). In this process, the desired DNA or RNA molecules that will target the antigen of interest are isolated from a large library with random sequences.<sup>18</sup> Once isolated, the nucleic acid strands that show high affinity to the target are sequenced. Aptamer with this sequence can then be synthesized through standard solid phase synthesis processes, enabling rapid fabrication and the ability to functionalize the aptamer with fluorophores or linking molecules in a sequence specific manner. Although these molecules are newer to the field and have less history of use in research, they offer the advantage of being much easier to produce. In addition, aptamers are also more thermally stable since they can be reversibly denatured.

## 1.5. PEDOT Nanoparticle Functionalization

In order to encourage nanoparticles to bind preferentially to cancer cells, a targeting molecule that recognizes and binds to surface markers on cancer cells can somehow be attached to the surface of the nanoparticles. In this study, we will refer to this surface modification of the PEDOT nanoparticles as “functionalization” as it adds the function of targeted delivery to the nanoparticles. The overall goal of this study is to first synthesize PEDOT nanoparticles and then attempt to functionalize PEDOT nanoparticles with a targeting molecule, either of protein or nucleic acid origin, that will recognize and bind to cancer cells.

Four methods of functionalization were attempted. In each of these methods, different reactions and reagents were used to attempt to attach a targeting molecule to PEDOT nanoparticles. First, we investigated whether targeting molecules can be used to directly attach an amine-containing molecule to PEDOT nanoparticles by conjugation with the surfactant poly(4-styrenesulfonic acid-co-maleic acid) that is used during nanoparticle synthesis. Second, functionalization was attempted by a previously reported layer-by-layer assembly.<sup>19</sup> In this method, two different polymers, poly(allylamine hydrochloride) (PAH) and poly(acrylic acid) (PAA) were layered on top of PEDOT nanoparticles, followed by the attachment of a spacer poly(ethylene glycol) (PEG) molecule that can be reacted with a targeting molecule. Third, functionalization by ionic linking of a negatively-charged aptamer to positively-charged PAH-coated PEDOT nanoparticles was attempted. Finally, covalent functionalization was attempted by

layering PAH onto PEDOT nanoparticles, using the primary amine groups to attach a PEG spacer molecule, and then attaching an aptamer to the PEG.

## 2. MATERIALS AND METHODS

### 2.1 Materials

3,4-Ethylenedioxythiophene (EDOT) and hydroxylamine hydrochloride were purchased from Alfa Aesar (Ward Hill, MA, USA). 4-Dodecylbenzenesulfonic acid (DBSA) and 1-ethyl-3-(3-dimethylaminopropyl)carbodiimide (EDC) were purchased from Tokyo Chemical Industry (TCI) America (Portland, OR, USA). Poly(4-styrenesulfonic acid-*co*-maleic acid) (PSS-*co*-MA), iron (III) chloride, bovine serum albumin, poly(allylamine hydrochloride) (PAH), and poly(acrylic acid) (PAA) were purchased from Sigma-Aldrich (St. Louis, MO, USA). Chloroform and 12-14,000 kDa MWCO dialysis tubing were purchased from VWR Scientific (VWR Chemicals) (Radnor, PA, USA). 100 kDa MWCO dialysis membrane was purchased from Spectrum Chemical (New Brunswick, NJ, USA). N-hydroxysuccinimide (NHS), sodium hydroxide, and fluorescein isothiocyanate (FITC) were purchased from Thermo Fisher Scientific (Waltham, MA, USA). Phosphate buffered saline stock was purchased from SeraCare Life Sciences (Milford, MA, USA). MUC1 aptamer with sequence 5'-/56-FAM/GCA GTT GAT CCT TTG GAT ACC CTG FTT TTT/3AmMo/-3' and scrambled aptamer with sequence 5'/56-FAM/AGG TGC CTC TTA CGT TGA TCG GAC TTT TTT/3AmMO/-3' were purchased from Integrated DNA Technologies (Coralville, IA, USA). 50 KDa MWCO floating dialysis tubes were purchased from G-Biosciences (St.

Louis, MO, USA). Succinimidyl carbonate-poly(ethylene glycol)-carboxymethyl (SC-PEG-CM) was purchased from Laysan Bio (Arab, AL, USA). Dulbecco's modified eagle medium (DMEM) with and without calcium and magnesium and Penicillin/Streptomycin solution were purchased from Corning (Corning, NY, USA). Trypsin with ethylenediaminetetraacetic acid (EDTA) was purchased from Cytiva (Marlborough, MA, USA). 100 kDa MWCO Microsep Advance Omega centrifugal devices were obtained from Pall Corporation (Port Washington, NY, USA). 2-(N-Morpholino)ethanesulfonic acid monohydrate (MES) was purchased from Angus Chemical Company (Buffalo Grove, IL, USA). MCF-7 Breast Cancer cells were obtained from American Type Tissue Culture Collection (ATCC, Manassas, VA, USA) and donated by the laboratory of Dr. Karen Lewis at Texas State University.

## **2.2 PEDOT Nanoparticle Synthesis & Characterization**

PEDOT nanoparticles were prepared using an oxidative emulsion polymerization of the monomer EDOT (**Figure 1**). Emulsion polymerization involves the mixing of an aqueous phase and organic phase to form monomeric nanodroplets with the aid of surfactants which are further polymerized *in situ*. The organic phase was prepared by adding 300 mg of 4-dodecylbenzenesulfonic acid (DBSA, 919  $\mu\text{mol}$ ) to 3 microcentrifuge tubes. Three more tubes were then prepared, each containing 3.6  $\mu\text{L}$  of EDOT (4.79 mg, 0.337 mmol) and 96.4  $\mu\text{L}$  of chloroform. The EDOT/chloroform solutions were then added to the microcentrifuge tubes containing DBSA and mixed using an Eppendorf ThermoMixer at 1400 RPM at room temperature for 30 minutes. The

aqueous phase was prepared by taking three glass vials and adding 20 mg PSS-co-MA (1  $\mu\text{mol}$ ) to each. 1 mL of ultrapure water was then added to each vial to create a 2% w/v solution of PSS-co-MA. The emulsion was formed by adding the organic phase into the aqueous phase dropwise with magnetic stirring. An additional 2 mL of ultrapure water was added to each emulsion-containing vial to dilute the emulsion, and then the mixtures were sonicated with a Symphony VWR sonicator at room temperature for 1 minute. The mixtures were then allowed to stir for 30 minutes. Next, a 100 mg/mL aqueous solution of  $\text{FeCl}_3$  was prepared and 7.6  $\mu\text{L}$  of it (0.76  $\mu\text{g}$ , 4.7  $\mu\text{mol}$ ) was added to each vial, followed by stirring for 1 hour. The three vials were combined into a 100 kDa molecular weight cutoff dialysis bag from Spectrum Chemical (product number 131420) and dialyzed for 14-17 hours.

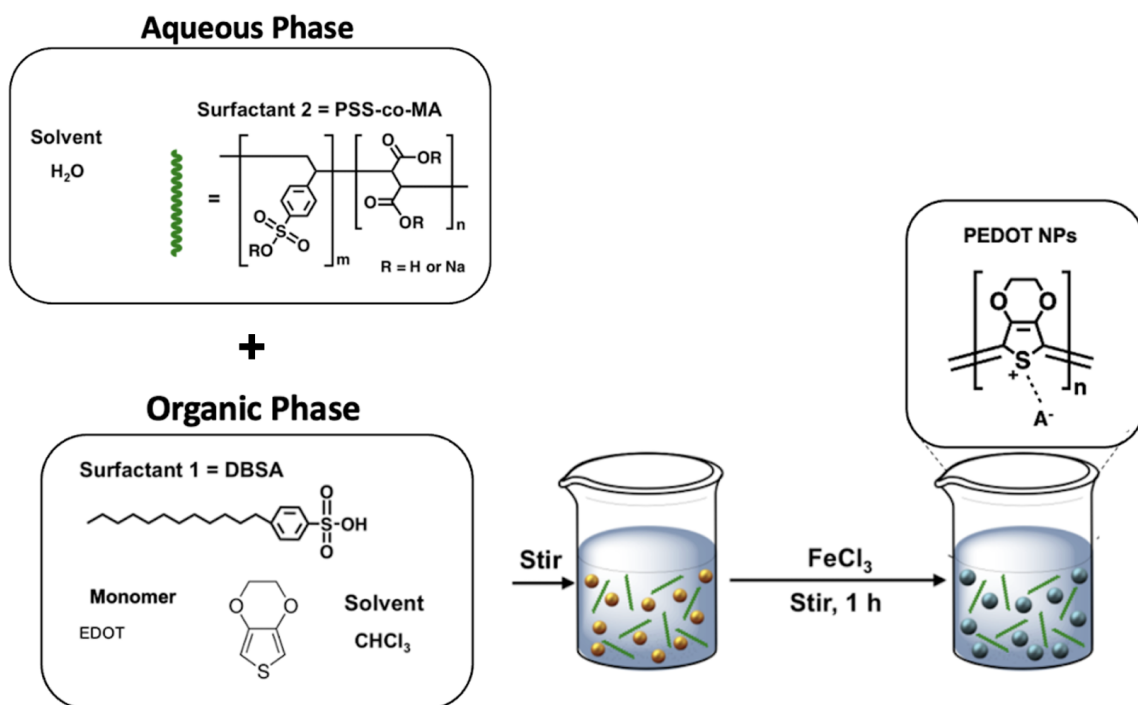


**Figure 1:** PEDOT nanoparticle synthesis. The organic phase consisting of the monomer EDOT and the DBSA surfactant is combined with the aqueous phase consisting of water

and the surfactant PSS-co-MA to form an emulsion. FeCl<sub>3</sub> then acts as an oxidizing agent to induce polymerization.

PEDOT nanoparticles were characterized using UV/VIS/NIR absorption spectroscopy to determine their absorbance in the NIR region. Using a Malvern Zetasizer Nano ZS instrument, their size was then determined by dynamic light scattering and their zeta potential was measured to learn about their surface charge. For dynamic light scattering, 300 μL of the nanoparticle suspension was added to a cuvette and analyzed. Zeta potential of the particles was analyzed by combining 100 μL of the nanoparticle suspension with 900 μL of 1 mM KCl solution.

The concentration of the PEDOT nanoparticles was estimated based on previous research group members' studies. In these studies, PEDOT nanoparticles were freeze dried and their mass obtained and compared to the original volume to determine concentration. The average mass per volume was 8.26 mg/mL. Since the final volume of each batch of PEDOT nanoparticles is around 9 mL, it was estimated that each batch contained 74.35 mg of nanoparticles. Since this is higher than the mass of EDOT used in the PEDOT nanoparticle synthesis, it can be concluded that the nanoparticles are composed of both PEDOT and surfactant (mostly DBSA because of the high mass used in the synthesis). This is as expected as the positively charged PEDOT polymer needs to be stabilized with the negatively charged surfactant to be maintained in its oxidated form.

### **2.3. Carbodiimide Functionalization**

Functionalization of PEDOT nanoparticles was attempted using carbodiimide chemistry on the maleic acid (MA) functional groups present in the PSS-co-MA

surfactant of the nanoparticles (**Figure 2**). First, to activate the carboxylic acid groups of MA, 3.03 mL of PEDOT nanoparticle suspension with a theoretical content of 333 nmol of PSS-co-MA and therefore 15.5  $\mu\text{mol}$  of maleic acid and 31  $\mu\text{mol}$  of carboxylic acids (see Appendix A for calculation) was added into 1.25 mL 0.05 M 2-(N-morpholino)ethanesulfonic acid (MES) (pH 6) coupling buffer. 25 mg (130  $\mu\text{mol}$ ) of 1-ethyl-3-(3-dimethylaminopropyl)carbodiimide (EDC) and 25 mg (220  $\mu\text{mol}$ ) of N-hydroxysuccinimide (NHS) were added to the solution, and then the reaction was allowed to take place for 15 minutes. The particles were then quickly washed two times with the coupling buffer using Microsep Advance 100 kDa MWCO centrifugal concentrators from Pall Corporation and resuspended. The particles were then coupled with bovine serum albumin labeled with FITC (BSA-FITC).

BSA-FITC was synthesized by first combining 2 g of BSA (30  $\mu\text{mol}$ ) with 234 mg (600  $\mu\text{mol}$ ) of FITC in 80 mL carbonate buffer (pH 9.0). This solution was allowed to stir overnight. Next, BSA-FITC solution was dialyzed using Spectra/Por dialysis tubing from VWR Scientific (12-14,000 kDa MWCO, product number 25225-260) in carbonate buffer until no FITC fluorescence was observed in the supernatant (excitation = 480 nm, emission = 520 nm). Then, the BSA-FITC was dialyzed in DI water to remove the salts from the carbonate buffer. The concentration of BSA-FITC was then determined using absorbance spectroscopy, specifically looking at absorbance of the protein at 280 nm. First, the absorbance of water was measured as a blank. Next, the absorbance spectrum of the BSA-FITC solution in water was measured. The value of the blank absorbance at 280 nm was then subtracted from the value of BSA-FITC absorbance at 280 nm. This

corrected absorbance was then used in the Beer-Lambert law equation with the extinction coefficient of 43824 to determine that the concentration of the BSA-FITC solution was 0.271  $\mu\text{mol/mL}$ . The BSA-FITC was then aliquoted into small containers and stored at  $-25^{\circ}\text{C}$ .

In order to facilitate successful conjugation and prevent crosslinking, the molar amount of MA within PEDOT nanoparticles needed to be estimated in order to then be able to estimate what a 5x molar excess of BSA-FITC would be. The molar amount of MA within PEDOT nanoparticles was estimated by first determining the molar amount of MA within the surfactant PSS-*co*-MA. PSS-*co*-MA consists of a 3:1 ratio of PSS groups to MA groups. The MW of one unit of PSS is 206 g/mol and the MW of one unit of MA is 116 g/mol. Therefore, proportionally, 15.8% of the molar mass of PSS-*co*-MA is MA. 20 mg (1  $\mu\text{mol}$ ) of PSS-*co*-MA was added to the PEDOT nanoparticle solution as a surfactant, meaning that 46.5  $\mu\text{mol}$  of MA and 92.9  $\mu\text{mol}$  of carboxylic acids were added and available for reaction. For the sake of this estimate, it was assumed that all of the MA was retained when the nanoparticles were formed, and none was washed out during dialysis. In this experiment, 3 mL of the PEDOT NPs (i.e. 33% of the batch, 0.333  $\mu\text{mol}$  PSS-*co*-MA, 15.5  $\mu\text{mol}$  of MA and 31  $\mu\text{mol}$  of carboxylic acids) were used. See Appendix A for calculations.

A volume of 4.18 mL of 0.271  $\mu\text{mol/mL}$  BSA-FITC solution (1133  $\mu\text{mol}$ , i.e. 3.7 BSA-FITC for every 100 carboxylic acids from maleic acid) was added to 1.25 mL coupling buffer. This solution was combined with the particles, mixed thoroughly, and allowed to react at room temperature for 2-4 hours with magnetic stirring and covered

from light. The low molar ratio of BSA-FITC to carboxylic acids from maleic acid used is reasonable based on the fact that not all the PSS-co-MA stays with the nanoparticles and that not all the carboxylic acid functional groups from the adsorbed polymer would be available on the surface; in addition, steric hindrance would prevent multiple BSA-FITC molecules from attaching to neighboring carboxylic acid functional groups. Particles were then washed with coupling buffer in 100 kDa MWCO Microsep Advance centrifugal devices from Pall Corporation and resuspended in the same buffer containing 25 mM of hydroxylamine to quench the reaction. The particles were washed once more and then resuspended in PBS for storage. Efficacy of this functionalization method was assessed using zeta potential and UV/VIS/NIR absorbance and fluorescence spectroscopy.

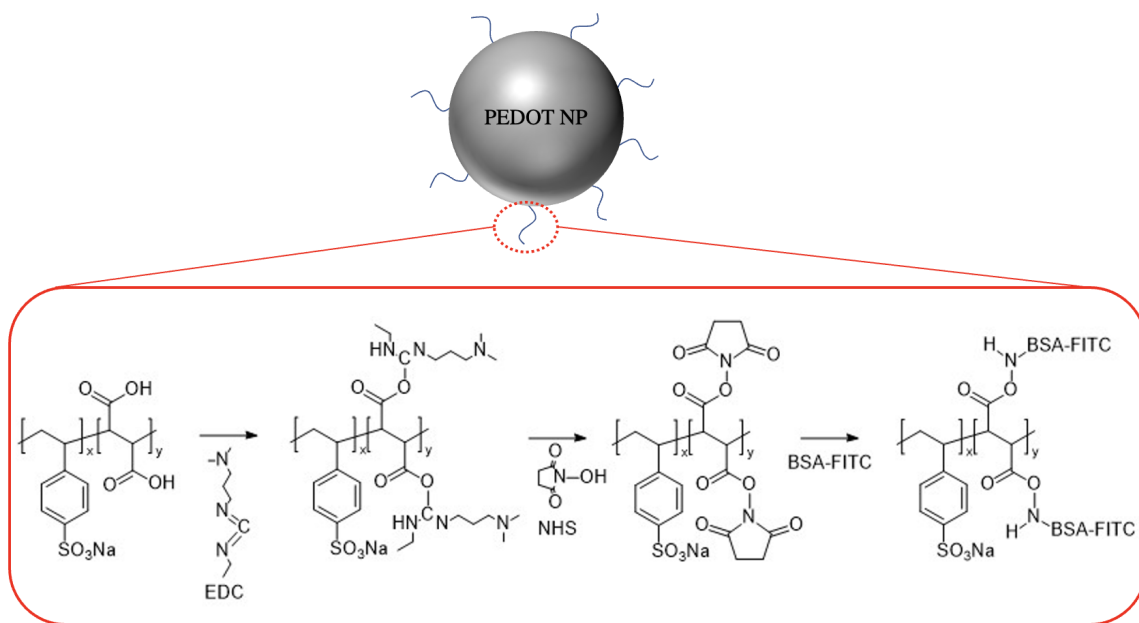


**Figure 2:** Schematic of the carbodiimide functionalization method. Surface COOH groups presumably available from surface-bound PSS-co-MA would be conjugated to BSA-FITC using EDC and NHS.

## 2.4 Layer-By-Layer Assembly Functionalization

Functionalization by layer-by-layer assembly of polymer-coated PEDOT nanoparticles using PAH and PAA followed by attachment of a spacer poly(ethylene glycol) (PEG) molecule was attempted following the procedure detailed by Cheng et al.<sup>19</sup> This procedure first involved layering positively-charged PAH onto the negatively-charged PEDOT nanoparticles (**Figure 3**). In order to layer PAH onto PEDOT nanoparticles, 2 mL of PEDOT nanoparticle suspension was added dropwise to 4 mL of 1 mg/mL PAH solution under ultrasonication over the course of 30 minutes. This was then left to react overnight and subsequently purified by washing in a 100kDa MWCO centrifugal concentrator. Next, the obtained PEDOT-PAH nanoparticle suspension was added dropwise to 1 mL PAA under ultrasonication. The protocol was terminated at this point due to severe nanoparticle aggregation. If the aggregation had not occurred, the PAA polymer would likely have been layered on top of the PAH layer and the two layers could have been crosslinked using EDC/NHS. Next, a PEG molecule would likely have been covalently attached to the outer layer of PAA, followed by attachment of a targeting molecule to the PEG arm.

Despite the secondary layer of PAA causing aggregation, the first layer was determined to be useful for future studies, and so we wanted to confirm the presence of primary amines on the surface of the particles after layering of PAH. To do so, an assay with fluorescamine was performed. Fluorescamine is a molecule that is normally not fluorescent, but when reacted with a primary amine, it becomes fluorescent. First, a standard curve was produced by first performing a two-fold serial dilution of PAH in

water beginning with 0.2 mg/mL and diluting until fluorescence was not detectable (see Appendix B). Then, 75  $\mu\text{L}$  of each dilution was added to a 96-well plate, and 25  $\mu\text{L}$  of 3 mg/mL fluorescamine dissolved in acetone was added to each well. The fluorescence of each well was measured with an excitation of 365 nm and an emission of 490 nm. These fluorescence values were plotted against the known concentrations of PAH and the equation of the line was found (Appendix B).

To determine the concentration of PAH present in the PAH-coated PEDOT nanoparticle suspension, 75  $\mu\text{L}$  of the nanoparticle suspension was added to a well in a 96-well plate and then 25  $\mu\text{L}$  of 3 mg/mL fluorescamine dissolved in acetone was added. The fluorescence RFU value (excitation = 365 nm, emission 490 nm) was entered as the y value to the known equation of the line from the standard curve. The resulting x value was equal to the concentration.

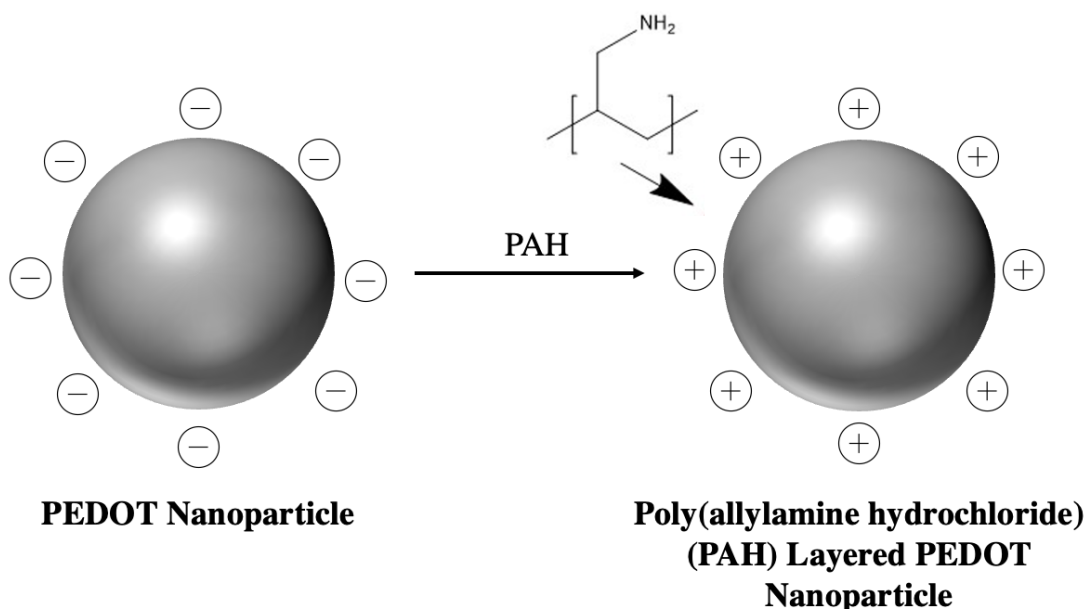


**Figure 3:** Schematic of PAH layering onto PEDOT nanoparticles. The negative charge of the PEDOT nanoparticles and the positive charge of the PAH interact.

## 2.5 Ionic Linking to PAH-Coated PEDOT Nanoparticles

Positively charged PAH-coated PEDOT nanoparticles were functionalized by ionic attachment to negatively-charged aptamer (**Figure 4**). First, 4  $\mu\text{L}$  of 100  $\mu\text{M}$  MUC1 aptamer dissolved in DI water was diluted in 196  $\mu\text{L}$  of autoclaved water. This mixture was then combined with 100  $\mu\text{L}$  of 3 mg/mL PAH-coated PEDOT nanoparticle suspension and allowed to react overnight. The product was purified by dialysis with a 50 kDa MWCO floating dialysis tube. Characterization was performed by measuring zeta potential and fluorescence with excitation at 480 nm.

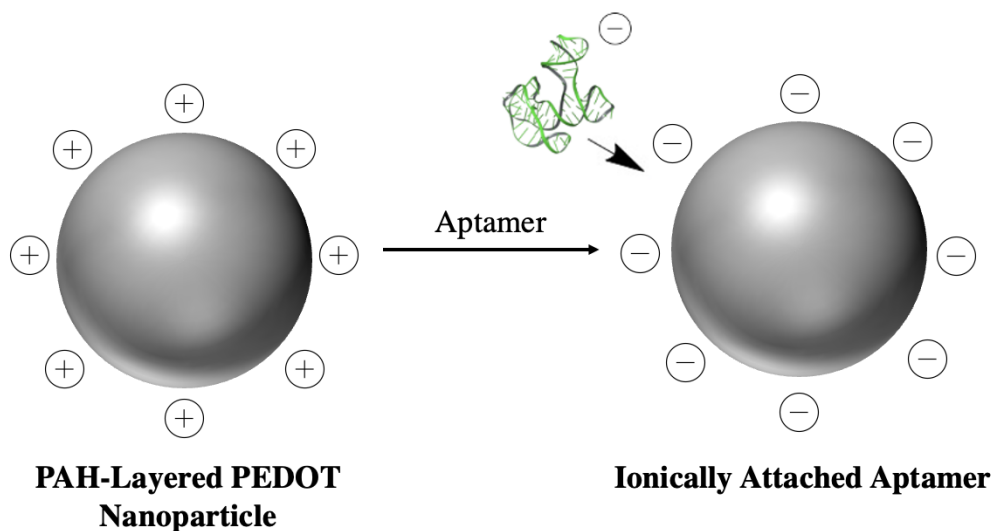


**Figure 4:** Schematic of ionic attachment of aptamer to PAH-coated PEDOT nanoparticles.

## 2.6 Covalent Linking to PAH-Coated PEDOT Nanoparticles using SC-PEG-CM

PAH-coated PEDOT nanoparticles were covalently linked to aptamer using a poly(ethylene glycol) (PEG) crosslinking molecule. PAH-coated PEDOT nanoparticles

were diluted to 3 mg/mL in ultrapure water. With mixing, 100 mg of succinimide-PEG-carboxymethyl (SC-PEG-CM) were added to the nanoparticle suspension and allowed to react overnight. Next, the pH was brought up to about 7 using NaOH. The succinimide end of the PEG molecule reacts with the primary amine groups present on the PAH (**Figure 5**). After reaction, the product was purified by dialysis with a 50 kDa MWCO floating dialysis tube, and the success of the reaction was assessed by measuring zeta potential.

To conjugate the PEGylated particles to aptamer, a carbodiimide reaction was induced between the carboxymethyl group on the PEG molecule on the surface of the nanoparticles and the amine group present on the MUC1 aptamer. First, 25 mg (0.13 mmol) of EDC and 30 mg (0.26 mmol) of NHS were dissolved in 1 mL of autoclaved water. Then, 4  $\mu$ L of MUC1 aptamer were diluted in 196  $\mu$ L of autoclaved water. This mixture was combined with 100  $\mu$ L of the PEGylated nanoparticle suspension and allowed to react overnight. The product was purified by dialysis with a 50 kDa MWCO floating dialysis tube. Characterization was performed by measuring zeta potential and fluorescence of the FAM label of the aptamer when excited at 480 nm.

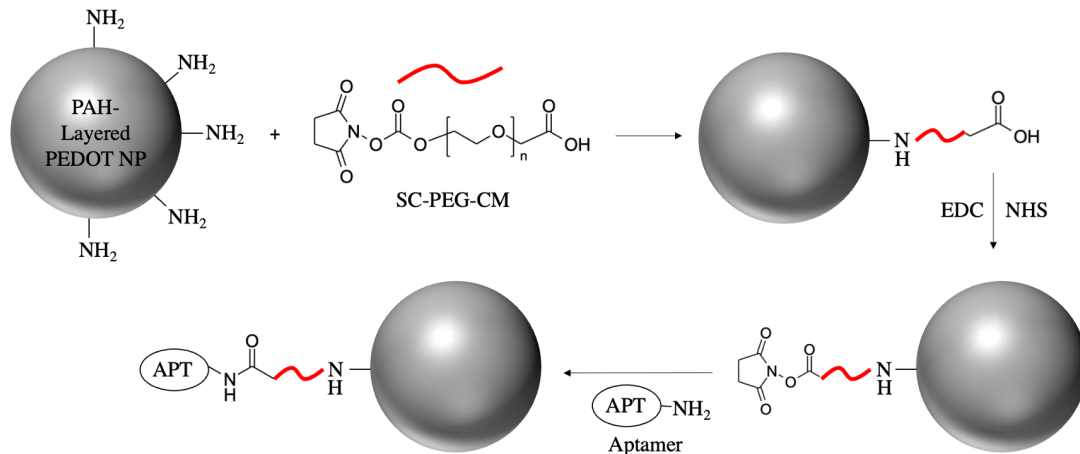


**Figure 5:** Schematic of covalent linking of PAH-coated PEDOT nanoparticles to aptamer using SC-PEG-CM.

### 3. RESULTS AND DISCUSSION

#### 3.1 PEDOT Nanoparticle Synthesis & Characterization

The synthesized PEDOT nanoparticles had an average size of 69.78 nm (Figure 6). This is within the optimal size range for use in the human body because particles of <100 nm are small enough to be able to evade the mechanisms of the immune system but large enough to stay within the body and not be cleared by the renal system.<sup>5</sup> The synthesized PEDOT nanoparticles also had a polydispersity index (PDI) of 0.298. PDI is a measurement of size distribution and ranges from 0 to 1. It is calculated by dividing the square of the standard deviation of nanoparticle sizes by the mean size of the nanoparticles. A higher PDI is indicative of more inconsistency in nanoparticle sizing. Ideally, a low PDI would be present for studies using PEDOT nanoparticles.

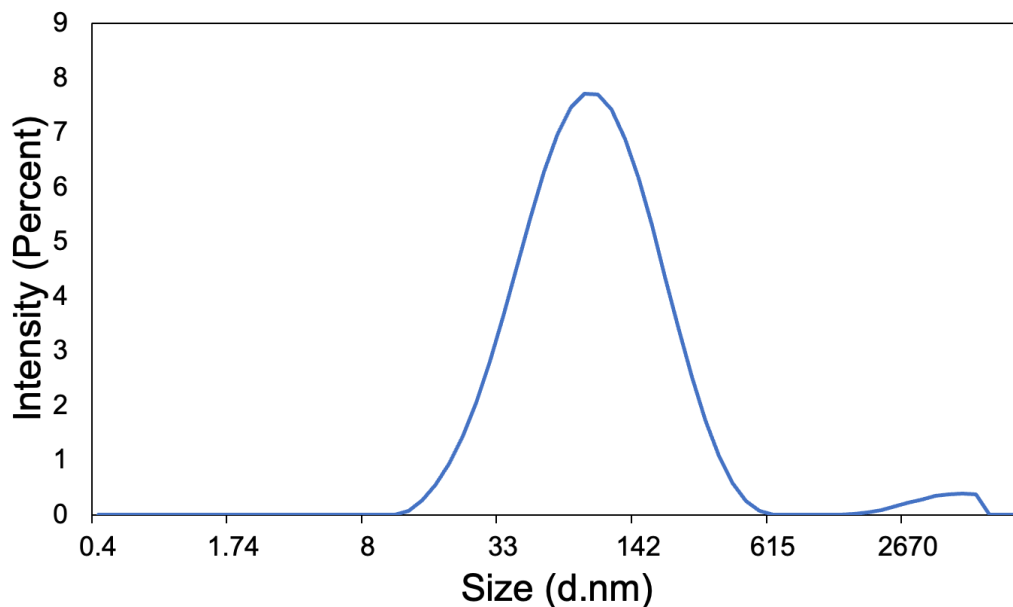


**Figure 6:** Size distribution of PEDOT nanoparticles measured by dynamic light scattering. The peak of the distribution is centered at 69.78 nm.

The average zeta potential of the synthesized PEDOT nanoparticles was  $-74.1 \pm 1.7$  mV. Zeta potential is a measure of the surface charge on particles. The highly negative zeta potential of PEDOT nanoparticles contributes to its high stability in aqueous suspension at room temperature. In addition, the PEDOT NPs were shown to absorb light in the NIR range with an optical density (OD) of nearly 1 (Figure 7). The peak absorption appears at around 775 nm, and absorbance is high at 808 nm, which is the wavelength of the laser that would ultimately be used for PTT studies.

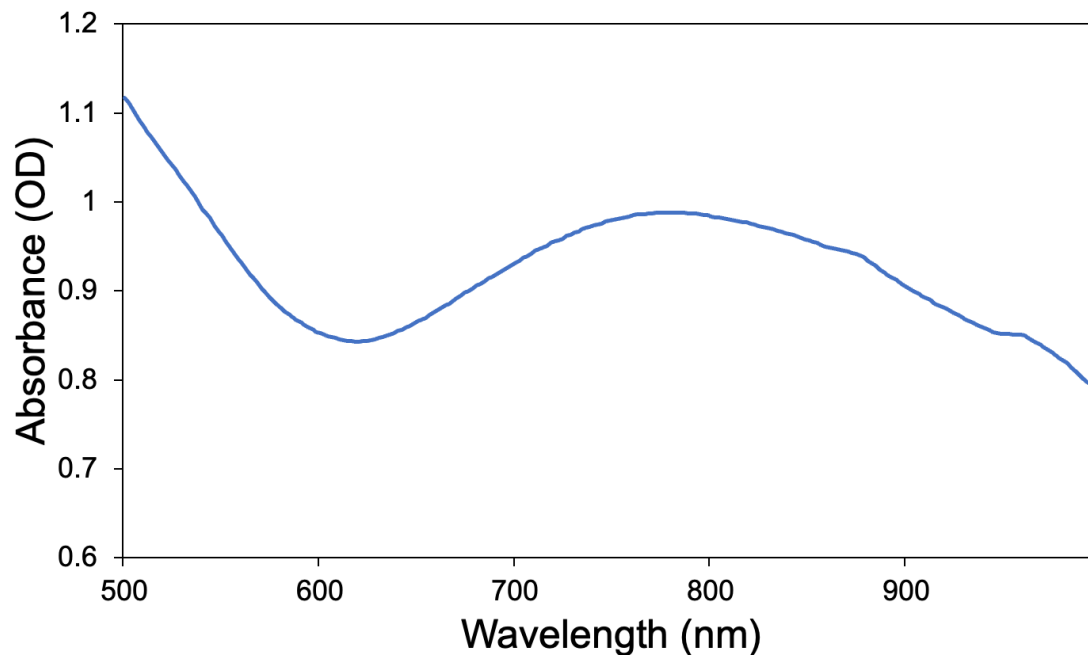


**Figure 7:** Absorption spectrum of PEDOT nanoparticles. The peak is around 775 nm, and absorption is still high at 808 nm, the wavelength of NIR lasers.

### 3.2 Carbodiimide Functionalization

PEDOT nanoparticles were reacted with fluorescently labeled BSA-FITC with the idea of utilizing carboxylic acid functional groups from PSS-co-MA that may have been permanently associated with the nanoparticles as anchors for carbodiimide-mediated linkage of the protein. Here, BSA-FITC acted as an inexpensive substitute to an antibody or aptamer that would be used for actual cancer cell-targeting purposes. Unfortunately, the absorbance spectra of the particles conjugated to BSA-FITC with EDC/NHS and the absorbance spectra of the control particles without EDC/NHS (i.e. the non-specific adsorption control) were not significantly different (**Figure 8**). The same trend was seen in the fluorescence data, with the two samples having similar results (**Figure 9**). This

indicates that similar amounts of BSA-FITC are present in both samples, meaning that covalent binding of BSA-FITC to MA groups in PEDOT nanoparticles did not occur.

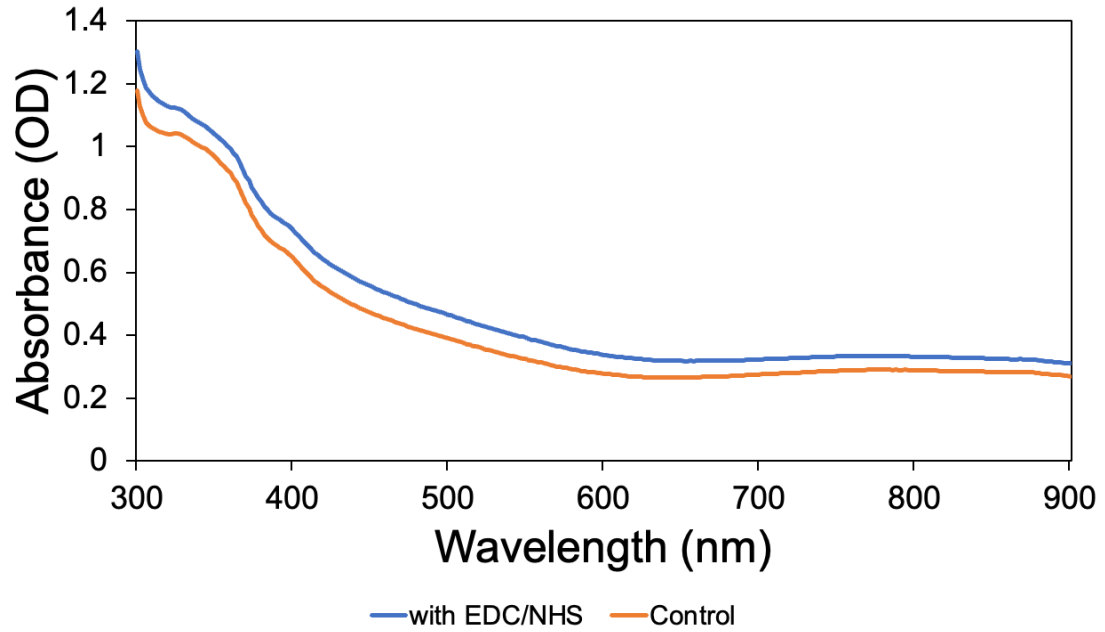


**Figure 8:** Absorbance of PEDOT nanoparticles conjugated to BSA-FITC with EDC/NHS and control sample with no EDC/NHS.

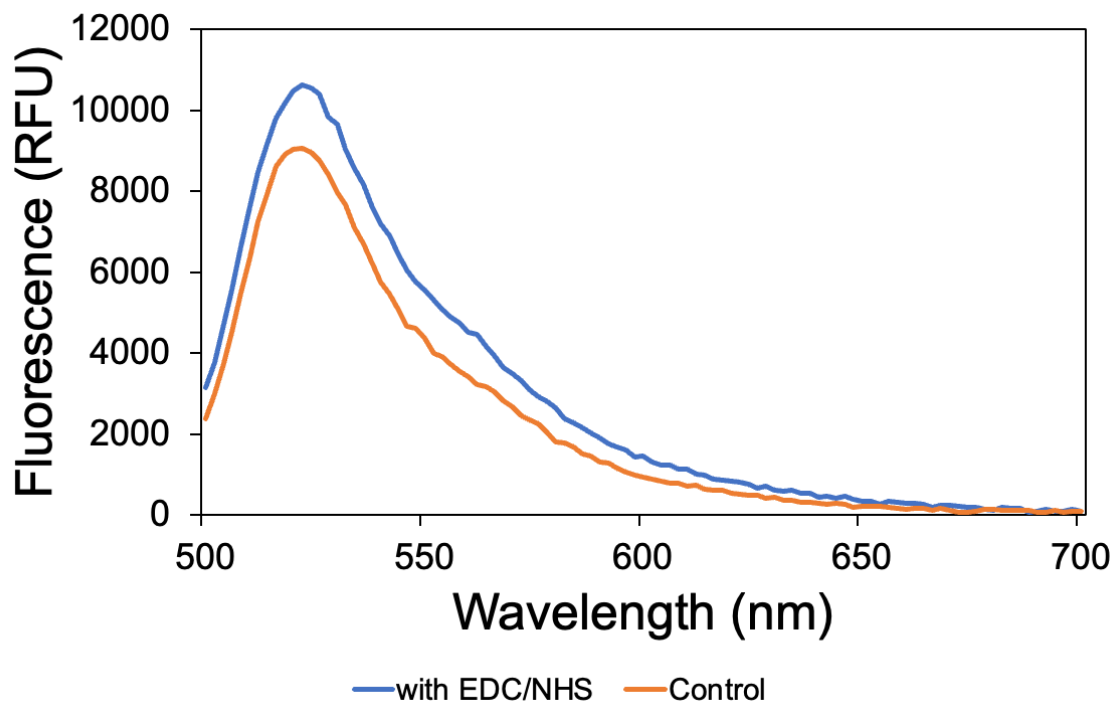


**Figure 9:** Fluorescence of PEDOT nanoparticles conjugated to BSA-FITC with EDC/NHS and control sample with no EDC/NHS.

A similar reduction in zeta potential was also seen in both samples (**Figure 10**).

The similarity of the zeta potentials again indicates that covalent binding between BSA-FITC and MA groups in PEDOT nanoparticles did not occur. The overall reduction in zeta potential is likely due to either the decreased presence of surfactants in the PEDOT nanoparticle suspensions due to the washing that occurred during the procedure or to non-specific adsorption of BSA-FITC to the surface.

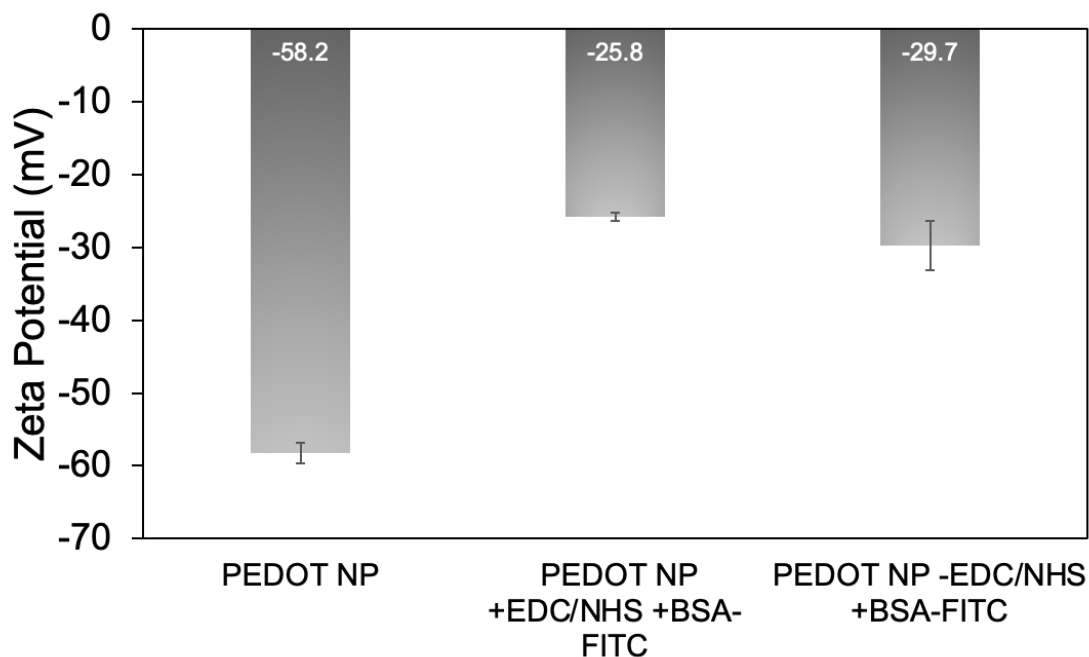


**Figure 10:** Zeta potential of control PEDOT nanoparticles and PEDOT nanoparticles reacted with BSA-FITC with and without EDC/NHS.

Overall, these results indicate that MA functional groups are not present on the surface of PEDOT nanoparticles in sufficient concentration and therefore are not available to covalently bind to targeting molecules. In the future, the presence or absence of MA functional groups could be confirmed by performing a titration with PEDOT nanoparticles.

### 3.3 Layer-By-Layer Assembly Functionalization

For layer-by-layer assembly functionalization, previous studies had demonstrated PEDOT nanoparticles being layered with PAH and then PAA, these layers being crosslinked, a PEG spacer molecule being covalently attached, and a targeting molecule being attached to the PEG arm. After PAH layering onto PEDOT nanoparticles, the zeta

potential increased from -46.93 mV to 58.67 mV (**Figure 11**). Unfortunately, when the PAH-coated PEDOT nanoparticle suspension was added to the PAA-containing solution, the nanoparticles aggregated and were not able to be resuspended. This aggregation may have been due to the particles becoming neutral in the process of being coated and thereby no longer repelling one another and aggregating. It could also have been due to PAA bridging particles together. To troubleshoot, different ratios and concentrations of PAH-coated PEDOT nanoparticle solution and PAA were used, but aggregation occurred regardless of these changes.

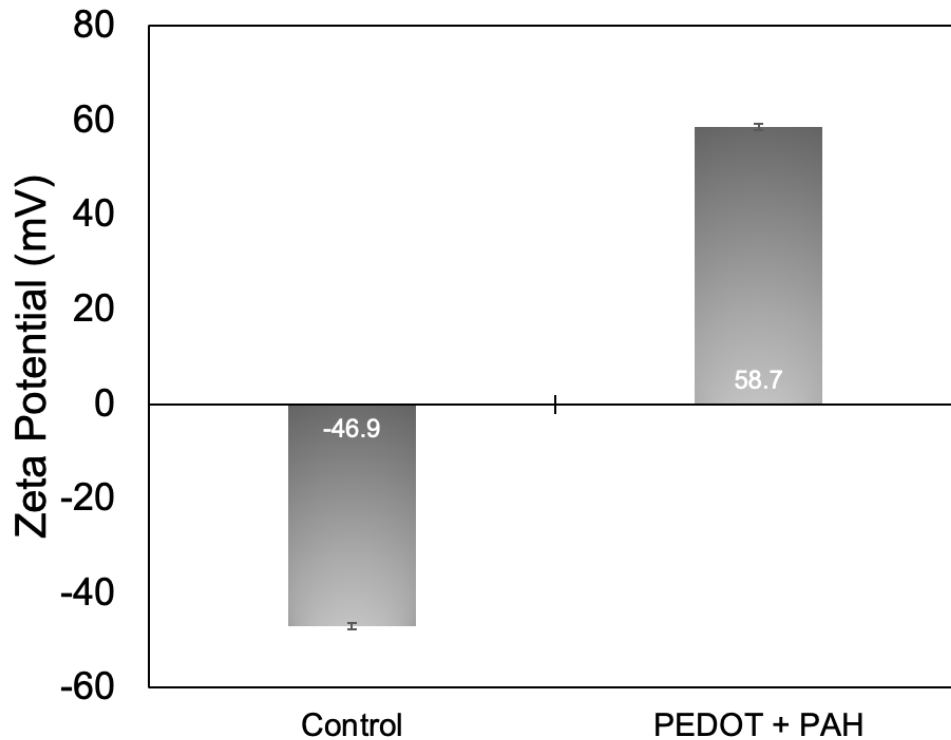


**Figure 11:** Zeta potential of control PEDOT nanoparticles and PAH-coated PEDOT nanoparticles.

Because of the aggregation, the layer-by-layer assembly functionalization method is not viable for these nanoparticles. However, the layering of PAH onto PEDOT

nanoparticles offers many advantages for subsequent functionalization trials. First, the high zeta potential of the PAH-coated PEDOT nanoparticles means that the particles are highly stable at room temperature in aqueous solution. In addition, PAH has primary amine groups in its structure. With PAH layered on top of PEDOT nanoparticles, the PEDOT nanoparticles are now covered in primary amine groups available for covalent bonding through alternate chemical reactions.

### **3.4 Ionic Linking to PAH-Coated PEDOT Nanoparticles**

PAH-layered PEDOT nanoparticles have a positive surface charge due to the positive charge of the PAH. The targeting molecule in use for this method, aptamers, are made of DNA and are therefore negatively charged. Since opposite charges attract, negatively-charged aptamer was added to the positively-charged particles and allowed to ionically interact. After mixing the PAH-coated PEDOT nanoparticles with the aptamer, the zeta potential went from positive to negative (**Figure 12**). This indicates that the negatively-charged aptamer is present on the surface of the nanoparticles.

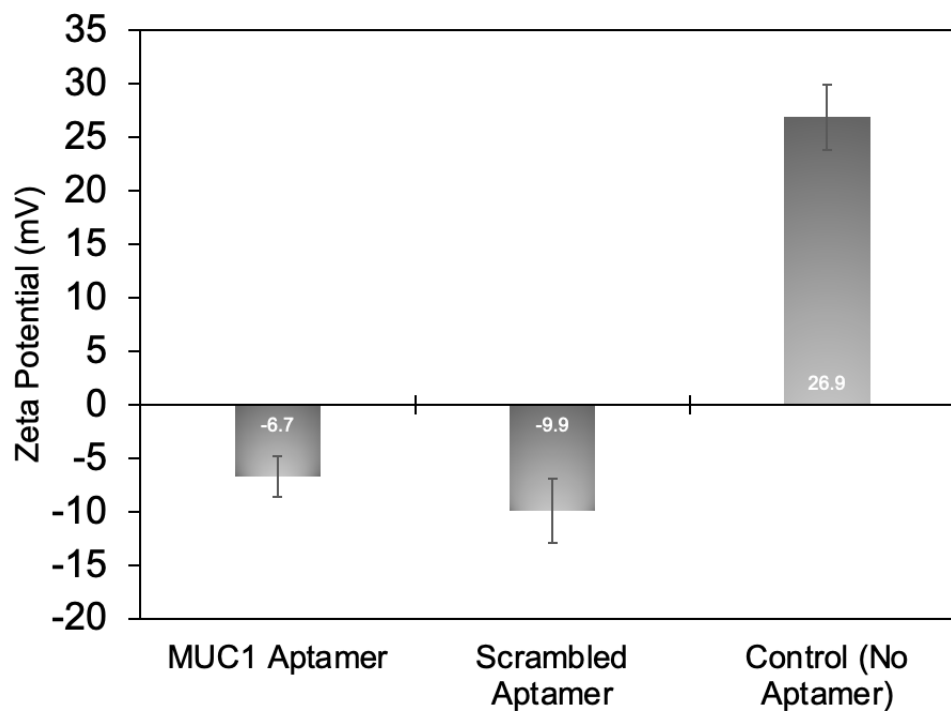


**Figure 12.** Zeta potential of PAH-coated PEDOT nanoparticles with ionically attached aptamer.

These results show that aptamer seems to be ionically linking to the nanoparticles. However, functionalizing the PEDOT nanoparticles in this way may have a few drawbacks. First, it is possible that the aptamer is laying flat on the nanoparticle rather than being attached in a way that enables binding to the aptamer's target. Second, ionic interactions, unlike covalent attachment, have the potential to be disrupted by things such as change in pH. This method of functionalization may not be stable enough for use in the body for PTT. However, it could potentially have other uses in which pH change or other forces that could disrupt ionic interaction will not play a factor.

### 3.5 Covalent Linking to PAH-Coated PEDOT Nanoparticles using SC-PEG-CM

PAH contains many primary amine groups available for covalent linking. With PAH layered on top of PEDOT nanoparticles, the succinimide end of an SC-PEG-CM spacer molecule was reacted with these primary amines and the carboxylic acid side of the molecule was reacted to the amine-containing aptamer using EDC/NHS (**Figure 5**). First, the success of the attachment of the PEG spacer molecule was assessed by zeta potential. The PAH-coated PEDOT nanoparticle begins as positive due to the charge on the PAH. The PEG molecule is negatively charged due to the carboxylic acid group present. After reacting the particles with the PEG molecule, the zeta potential changed from positive to negative (**Figure 13**).

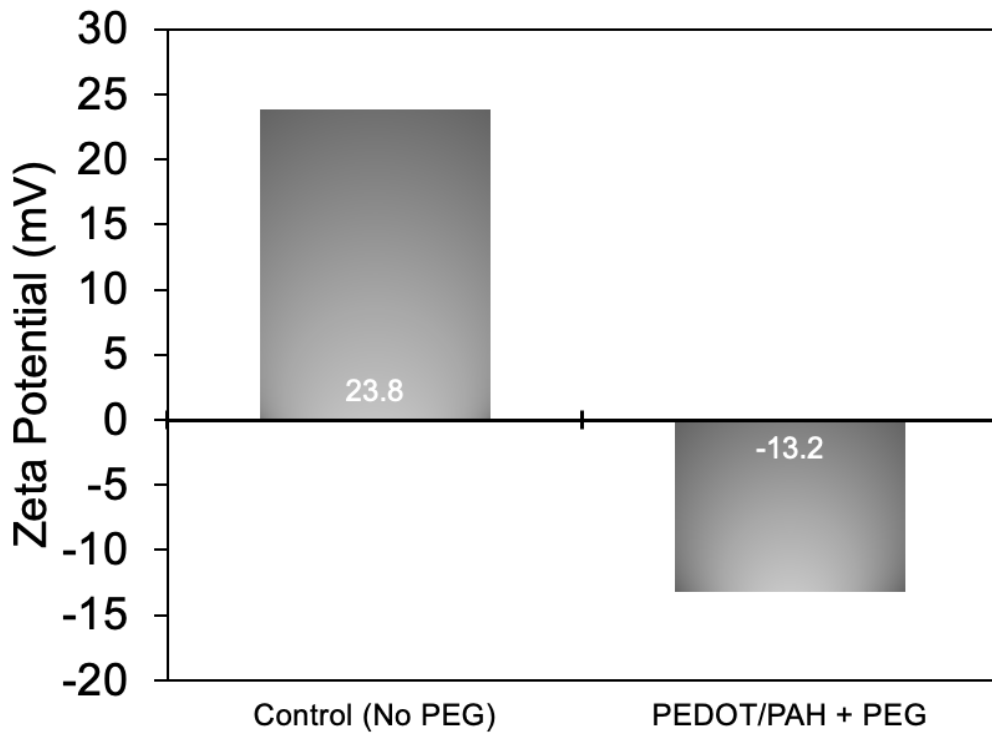


**Figure 13.** Zeta potential of PAH-coated PEDOT nanoparticles after PEG attachment and control with no PEG attachment.

Following PEG attachment to the particles, aptamer was attached to the other end of the PEG molecules. The results were assessed by zeta potential and fluorescence spectroscopy. Since the aptamer is negatively charged, we would expect to see the zeta potential of the particles shifting to more negative values if aptamer was covalently attached. **Figure 14** shows the zeta potential results after covalent attachment. The control with no aptamer had a zeta potential of -7.3 mV. The controls that were reacted with aptamer but without the reagents EDC/NHS showed zeta potentials generally within the same range as the control without aptamer, indicating no covalent attachment. The samples reacted with aptamer (either anti-MUC1 or the scrambled control) and EDC/NHS had a zeta potential of -16.1 mV and -15.3 mV. These being more negative than the controls indicates successful covalent attachment.

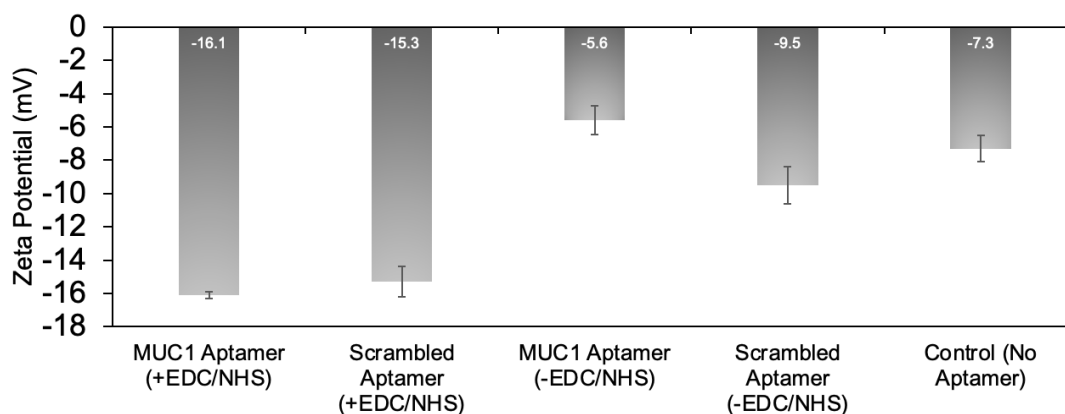


**Figure 14.** Zeta potential of PAH-coated PEDOT nanoparticles following covalent attachment of aptamer.

#### 4. CONCLUSIONS & FUTURE WORK

Nanoparticle-mediated PTT has shown to be a promising method for cancer treatment, and PEDOT nanoparticles in particular offer many benefits for usage in this

treatment. The identification of a method for functionalizing PEDOT nanoparticles that can be generalized to attach different targeting molecules in order to target different cancer cell types will be important to increase the efficacy of PEDOT nanoparticle-mediated PTT. This data shows that ionic attachment and covalent attachment show promise as methods of functionalizing PEDOT nanoparticles with targeting molecules. However, this data is preliminary and studies should be repeated.

Future work on this project includes further exploring the properties of functionalized particles as well as exploring the generalizability of the functionalization method. The next step for this project would be to subject the functionalized PEDOT nanoparticles to a cellular internalization study to determine whether or not they are able to bind preferentially to the MCF-7 cells that overexpress MUC1. This could be carried out by incubating the cells with particles functionalized using different methods, washing out unbound particles and aptamer, and observing the fluorescence of the FAM label of the aptamer associated with the cells. To further investigate whether particles are bound preferentially to cancer cells after functionalization, it would be beneficial to irradiate cells treated with functionalized PEDOT nanoparticles and observe which formulation leads to increased cell damage. In addition, the stability of functionalized nanoparticles should be investigated. This is especially for the ionic functionalization method as the lack of covalent bonding is likely to lead to less stable functionalization. Another method to learn more about the interaction of the functionalized nanoparticles would be looking at the internalization and intracellular localization of the particles using confocal microscopy. Finally, the generalizability of the identified functionalization methods could

be assessed by attaching different targeting molecules to the PEDOT nanoparticles that are able to bind to different cell lines.

Apart from their potential for usage in PTT, functionalized PEDOT nanoparticles could be used for other projects currently in progress within our research group. One potential use is in a project exploring photothermally responsive hydrogels as drug delivery systems. PEDOT nanoparticles will be incorporated into the matrix that forms these gels, and upon irradiation with a NIR laser, the PEDOT nanoparticles will heat and cause dynamic bonds within the matrix to break and then reform upon cooling. By functionalizing the PEDOT nanoparticles, we could ensure that they were better incorporated into the hydrogel matrix and in a more targeted fashion.

Another ongoing research project within our group is the development of a photothermal biosensor using PEDOT nanoparticles. The purpose of this biosensor as a medical device would be to rapidly detect the presence of a disease-related antigen in a patient's serum or other fluid. An antibody or aptamer that binds this antigen would be immobilized on the surface of the biosensor, and following the addition of the patient serum, photothermal nanoparticles functionalized with a targeting molecule recognizing the antigen will be added to the biosensor so as to form a sandwich immunoassay not unlike those used for ELISA assays or even pregnancy tests. Upon irradiation with a laser, the amount of antigen bound by the nanoparticles, and therefore the amount of antigen presence, can be quantified by measuring the change in temperature. Currently, a different type of photothermal nanoparticle is being used for this project, but a problem is that these nanoparticles are not photostable because the photothermal component of them

degrades quickly and therefore the particles do not stay heated.<sup>13</sup> PEDOT nanoparticles, however, stay heated as long as they are irradiated due to their high photostability. Identifying a functionalization method for PEDOT nanoparticles will allow for them to be used in this project.

## References

1. Cancer Facts & Figures 2021 | American Cancer Society  
<https://www.cancer.org/research/cancer-facts-statistics/all-cancer-facts-figures/cancer-facts-figures-2021.html> (accessed 2021-11-19).
2. FastStats <https://www.cdc.gov/nchs/fastats/leading-causes-of-death.htm> (accessed 2021-11-19).
3. Ahmad, F. B.; Anderson, R. N. The Leading Causes of Death in the US for 2020. *JAMA* **2021**, *325* (18), 1829–1830. <https://doi.org/10.1001/jama.2021.5469>.
4. Chemotherapy Side Effects  
<https://www.cancer.org/treatment/treatments-and-side-effects/treatment-types/chemotherapy/chemotherapy-side-effects.html> (accessed 2021-11-19).
5. Kaur, P.; Aliru, M. L.; Chadha, A. S.; Asea, A.; Krishnan, S. Hyperthermia Using Nanoparticles – Promises and Pitfalls. *International Journal of Hyperthermia* **2016**, *32* (1), 76–88. <https://doi.org/10.3109/02656736.2015.1120889>.
6. Cheng, L.; Wang, C.; Feng, L.; Yang, K.; Liu, Z. Functional Nanomaterials for Phototherapies of Cancer. *Chem. Rev.* **2014**, *114* (21), 10869–10939.  
<https://doi.org/10.1021/cr400532z>.
7. Huang, X.; Jain, P. K.; El-Sayed, I. H.; El-Sayed, M. A. Plasmonic Photothermal Therapy (PPTT) Using Gold Nanoparticles. *Lasers Med Sci* **2007**, *23* (3), 217.  
<https://doi.org/10.1007/s10103-007-0470-x>.
8. Nanospectra Biosciences, Inc. *A Pilot Study of AuroLase(Tm) Therapy in Patients With Refractory and/or Recurrent Tumors of the Head and Neck*; Clinical trial registration NCT00848042; clinicaltrials.gov, 2016.
9. Rastinehad, A. R.; Anastos, H.; Wajswol, E.; Winoker, J. S.; Sfakianos, J. P.; Doppalapudi, S. K.; Carrick, M. R.; Knauer, C. J.; Taouli, B.; Lewis, S. C.; Tewari, A. K.; Schwartz, J. A.; Canfield, S. E.; George, A. K.; West, J. L.; Halas, N. J. Gold Nanoshell-Localized Photothermal Ablation of Prostate Tumors in a Clinical Pilot Device Study. *PNAS* **2019**, *116* (37), 18590–18596.  
<https://doi.org/10.1073/pnas.1906929116>.
10. Yu, J.; Yang, L.; Yan, J.; Wang, W.-C.; Chen, Y.-C.; Chen, H.-H.; Lin, C.-H. Carbon Nanomaterials for Photothermal Therapies. In *Carbon Nanomaterials for Bioimaging, Bioanalysis, and Therapy*; John Wiley & Sons, Ltd, 2019; pp 309–340.

- <https://doi.org/10.1002/9781119373476.ch12>.
11. Hoffman, H. A.; Chakrabarti, L.; Dumont, M. F.; Sandler, A. D.; Fernandes, R. Prussian Blue Nanoparticles for Laser-Induced Photothermal Therapy of Tumors. *RSC Adv.* **2014**, *4* (56), 29729–29734. <https://doi.org/10.1039/C4RA05209A>.
  12. Wang, S.; Chen, W.; Jiang, C.; Lu, L. Nanoscaled Porphyrinic Metal–Organic Framework for Photodynamic/Photothermal Therapy of Tumor. *ELECTROPHORESIS* **2019**, *40* (16–17), 2204–2210. <https://doi.org/10.1002/elps.201900005>.
  13. Heshmati Aghda, N.; Abdulsahib, S. M.; Severson, C.; Lara, E. J.; Torres Hurtado, S.; Yildiz, T.; Castillo, J. A.; Tunnell, J. W.; Betancourt, T. Induction of Immunogenic Cell Death of Cancer Cells through Nanoparticle-Mediated Dual Chemotherapy and Photothermal Therapy. *International Journal of Pharmaceutics* **2020**, *589*, 119787. <https://doi.org/10.1016/j.ijpharm.2020.119787>.
  14. Cantu, T.; Walsh, K.; Pattani, V. P.; Moy, A. J.; Tunnell, J. W.; Irvin, J. A.; Betancourt, T. Conductive Polymer-Based Nanoparticles for Laser-Mediated Photothermal Ablation of Cancer: Synthesis, Characterization, and in Vitro Evaluation. *IJN* **2017**, *12*, 615–632. <https://doi.org/10.2147/IJN.S116583>.
  15. Huff, M. E.; Gökmen, F. Ö.; Barrera, J. S.; Lara, E. J.; Tunnell, J.; Irvin, J.; Betancourt, T. Induction of Immunogenic Cell Death in Breast Cancer by Conductive Polymer Nanoparticle-Mediated Photothermal Therapy. *ACS Appl. Polym. Mater.* **2020**, *2* (12), 5602–5620. <https://doi.org/10.1021/acsapm.0c00938>.
  16. Moncada, D. M.; Kammanadiminti, S. J.; Chadee, K. Mucin and Toll-like Receptors in Host Defense against Intestinal Parasites. *Trends in Parasitology* **2003**, *19* (7), 305–311. [https://doi.org/10.1016/S1471-4922\(03\)00122-3](https://doi.org/10.1016/S1471-4922(03)00122-3).
  17. Jing, X.; Liang, H.; Hao, C.; Yang, X.; Cui, X. Overexpression of MUC1 Predicts Poor Prognosis in Patients with Breast Cancer. *Oncology Reports* **2019**, *41* (2), 801–810. <https://doi.org/10.3892/or.2018.6887>.
  18. Liu, Q.; Zhang, W.; Chen, S.; Zhuang, Z.; Zhang, Y.; Jiang, L.; LIN, J. S. SELEX Tool: A Novel and Convenient Gel-Based Diffusion Method for Monitoring of Aptamer-Target Binding. *Journal of Biological Engineering* **2020**, *14* (1), 1. <https://doi.org/10.1186/s13036-019-0223-y>.
  19. Cheng, L.; Yang, K.; Chen, Q.; Liu, Z. Organic Stealth Nanoparticles for Highly Effective *in Vivo* Near-Infrared Photothermal Therapy of Cancer. *ACS Nano* **2012**, *6*

(6), 5605–5613. <https://doi.org/10.1021/mn301539m>.

## Appendix A

### Calculations of PSS-co-MA Molar Concentration and BSA-FITC Molar Excess

The average molecular weight of the PSS-co-MA polymer is 20,000 g/mol. The ratio of PSS to MA in the polymer is 3:1, so based on one repeat unit being three PSS groups and one MA group, the molecular weight of one repeat unit is 430.54 g/mol. The number of repeat units was found by dividing the molecular weight of the polymer by the molecular weight of one repeat unit:

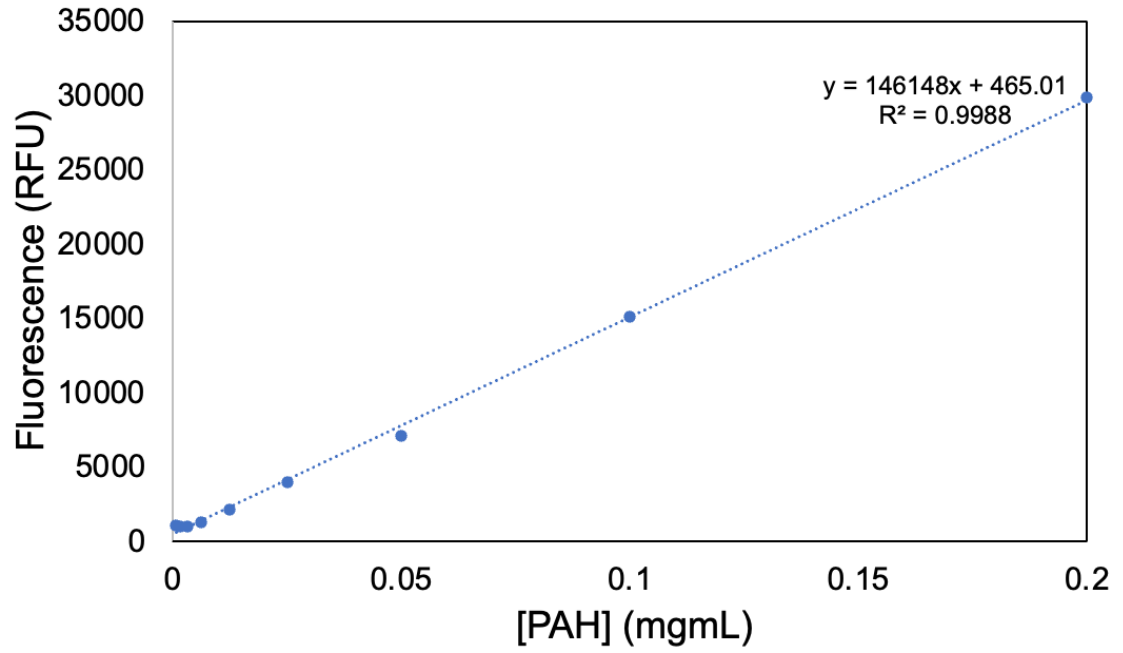
$$\frac{20,000 \text{ g/mol}}{430.54 \text{ g/mol}} = 46.45 \text{ repeat units}$$

Since there are two COOH groups in each MA, the number of COOH groups is equal to two times the number of repeat units, or 92.9. When synthesizing the nanoparticles, 20 mg of polymer was used, which is equal to 0.001 mmol of polymer. The molar amount of COOH groups in the polymer added during nanoparticle synthesis was determined by multiplying the molar amount of polymer used (0.001 mmol) by the number of COOH groups present in the polymer (92.9).

One third of the total nanoparticle batch was used for BSA-FITC attachment. Therefore, all molar amounts determined above were multiplied by  $0.\bar{3}$ . This means that  $0.\bar{3}$   $\mu\text{mol}$  of polymer, 15.48  $\mu\text{mol}$  of MA groups, and 30.97  $\mu\text{mol}$  of COOH groups were used for BSA-FITC attachment.

## Appendix B

### PAH and Fluorescamine Standard Curve



Excitation Wavelength: 382 nm

Emission Wavelength: 490 nm